ANSTO/E-746
ISBN 0-642-59993-9

Australian Nuclear Science and Technology Organisation

A SANS Study of the Adsorption of Guar Gum on Talc Surfaces

by

Sandra Leigh Cram, Robert Knott and Howard Hanley

Prepared within the Nanostructure of Complex Systems Project

October 2001

Abstract

Reagents based on guar gum are commonly used as 'gangue' depressants in the flotation of sulphides from ores containing naturally floating layer silicate minerals such as talc. Nickel sulphide ores processed by WMC Resources Ltd. at the Leinster Nickel Operations in Western Australia typically contain 1-2 % talc. Guar gum, added to the flotation cell, depresses the talc by adsorbing onto its surface, thereby reducing its hydrophobic nature. Guar gum is a long chain polysaccharide containing many hydroxyl functional groups along the length of its chain. The ratio of chain length to the number of hydroxyl and carboxyl groups causes the guar gum to be selective in depressing talc rather than nickel sulphide minerals.

Small angle neutron scattering (SANS) it is an excellent tool for probing structures in the nano length scale. Unlike X-rays, neutrons are sensitive to low atomic weight elements, especially hydrogen and therefore organics. Using SANS it is possible to contrast different parts of a composite sample to get information on spatial arrangements. These qualities make SANS an obvious choice for studying the adsorption of guar gum on the surface of talc in aqueous solutions.

Complimentary SANS experiments were carried out in Australia at the Australian Nuclear Science and Technology Organisation (ANSTO) and in the United States at the National Institute of Standards and Technology (NIST). Initially talc samples were studied 'as supplied', however as experiments proceeded attempts to reduce the particle size and distribution were carried out by milling and centrifuging procedures. Contrast matching techniques were used to observed the scattering behaviour of talc with and without the presence of guar gum and vice versa, over a total q range of 0.002 – 0.1 $Å^{-1}$. The size of the talc particles appears to affect the scattering behaviour not only of talc but also of guar gum in the same solutions. This implies that the structure of the guar gum is strongly influenced by the dimensions of the talc and could be taken as indirect evidence of adsorption of guar gum onto the talc surface.

Although adsorption has been implied, a model of the adsorption mechanism cannot be proposed from these preliminary results. In order to achieve this, more homogeneous talc samples need to be studied; in particular the poly dispersity of and impurities in the samples must be addressed.

1.0 Introduction and Background

Talc is a contaminant in the nickel ores processed by WMC Resources Ltd. at the Leinster Nickel Operations in Western Australia. The ore typically processed at this plant is a non oxidised nickel sulphide consisting of approximately 90% pentlandite and some millerite, the talc content is usually about 1 – 2%. Talc is a hydrous magnesium silicate mineral ($Mg_3Si_4O_{10}(OH)_2$) structurally composed of double layers of silica tetrahedrae sandwiched between single layers of brucite, $Mg(OH)_2$, Figure 1; as such it is classed as a 2:1 phyllosilicate [1,2].

The charge between brucite and the tetrahedral layers is zero and these layers are simply held together by van der Waals bonds. Since the ionic-electrostatic forces, which bind the ions within these layers, are much stronger than the bonding between the layers, cleavage preferentially occurs along these planes creating native hydrophobic mineral surfaces [3]. Conversely, the rupture of ionic or covalent bonds on the edges of the talc particle will form a polar surface, which is hydrophilic [3]. Preferential cleavage on the uncharged planes results in plate like particles with predominant hydrophobic behaviour.

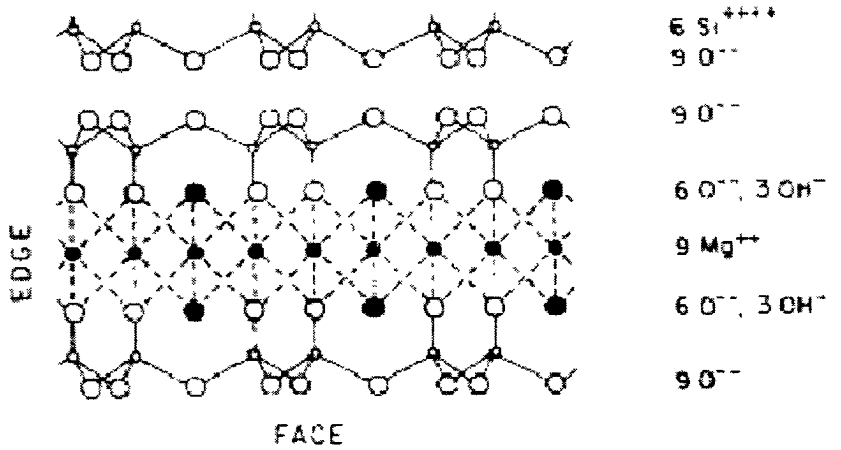

Figure 1 – Schematic of the face and edge views of talc [1]

A flotation method is used at the Leinster Nickel Operations to concentrate nickel ores. Flotation methods operate on the principle that collisions between hydrophobic particles and mechanically introduced air bubbles result in particle-bubble attachment. Nickel sulphide ores are naturally hydrophobic and therefore become concentrated in the froth at the top of the flotation cell. The addition of collector species, (sodium ethyl xanthates) enhances the hydrophobicity of the sulphide ores and frother agents (IF56 a commercial product based on methyl isothobutyl ketone) are used to increase the collection rate and removal of nickel ore from the cells [4]. The problem with talc is that it is also naturally hydrophobic and if not properly regulated the talc will also be recovered in the froth.

Guar gum is added to the flotation cell to depress the talc by adsorbing onto the talc surface, thereby reducing its hydrophobic nature. Guar gum is a long chain polysaccharide [3], (Figure 2) containing many hydroxyl functional groups along the length of its chain. As a natural product its molecular weight (MW) can be quite varied, but typically commercial samples have MWs of about 200,000 [5]. Whilst the ratio of chain length to the number of hydroxyl and carboxyl groups causes the guar gum to be selective in depressing talc rather than the nickel sulphide minerals [6], the quantities of guar gum added are carefully regulated to ensure that this balance is maintained [4].

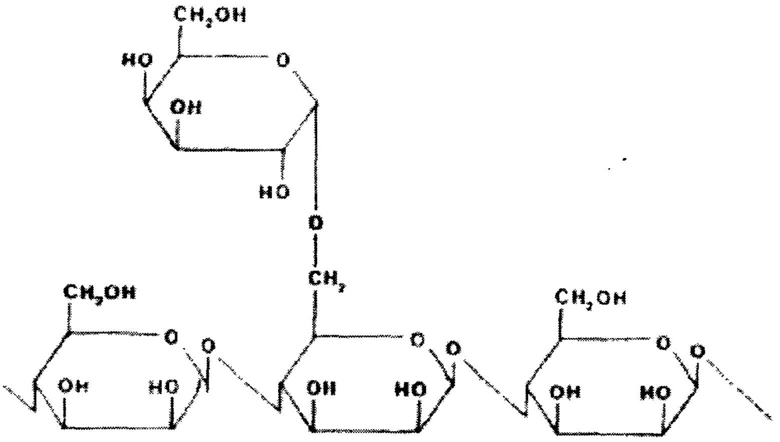

Figure 2 – the molecular structure of guar gum [3]

There are number of theories proposed on how guar gum adsorbs onto the surface of talc [3,6]. The most prominent involve hydrogen bonding on the edges of the talc and hydrophobic bonding on the faces of the talc. Hydrogen bonding occurs between charged silicon and magnesium oxides and hydroxides on the polar edges of the talc particles and the hydroxyl groups on the guar gum chain. Hydrophobic bonding occurs when the water molecules at the mineral surface with low polarity (i.e. the face of the talc), are displaced with polymeric species. Chemical interactions can also occur, for example between the carboxyl groups on the guar molecule and magnesium ions at the mineral edges. In some cases there might be coulombic interactions between ionised forms of guar and charged mineral interfaces, although this is not deemed to be an important mechanism in the present study. It is most probable that the adsorption occurs through a number of these mechanisms operating simultaneously [3,6]. Regardless of the exact mechanism responsible, it is clear that once adsorbed the OH groups on the polymer chain extend into the solution and render the coated particle as hydrophilic [3].

1.1 Objective

The aim of this project was to establish whether small angle neutron scattering (SANS) could observe the adsorption of guar gum on talc surfaces, and if so, what information about the adsorption behaviour could be retrieved.

SANS it is an excellent tool for probing structures in the nano length scale. Unlike X-rays, neutrons are sensitive to low atomic weight elements, especially hydrogen and therefore organics, they are also non-destructive and penetrating. Using SANS it is possible to contrast different parts of a composite sample to get information on spatial arrangements, for example, porosity, molecular structure, coatings or layering. These qualities make SANS very useful for studying organic samples in their natural environment, with little sample preparation required. SANS is therefore an obvious choice for studying the adsorption of guar gum on the surface of talc in aqueous solutions. Information gained from such a study could provide a model of surface interactions between guar gum and talc and this could ultimately be used to optimise the flotation process.

2.0 Experimental

2.1 Materials

2.1.1 Talc

Powdered talc samples were supplied by WMC Resources Ltd., with an X-ray diffraction (XRD) analysis, Table 1.

Table 1 – XRD analysis of raw talc powder

Mineral	Quantity
Talc ($Mg_3Si_4O_{10}(OH)_2$)	56%
Magnesite ($MgCO_3$)	37%
Serpentine ($A_3Si_2O_5$) Where A = Mg, Fe^{2+}, or Ni	4%
Pentlandite $(Ni, Fe)_9S_8$	trace

In addition a number of talc samples were milled in an attempt to reduce the natural particle size and distribution. In principle, a finer particle size would encourage the formation of a stable suspension in aqueous solutions and also facilitate SANS analysis. The milled samples were prepared by CSIRO, Division of Manufacturing Science and Technology, by a ball milling process using zirconia beads. The talc was milled in either water or an organic solvent 'Isopar L'. Milling in water was carried out both with and without an organic dispersant 'Orotan 731' . Milling in Isopar was always carried out with an organic dispersant 'Solsperse 2100'. Identical milling procedures were followed in each case, Table 2.

Table 2 – Details of the Milling process of talc samples conducted at CSIRO

Sample Description	Wt% solids
Raw Talc	100
Raw talc milled in H2O with no dispersant	25
Raw talc milled in H2O + 6wt% Orotan 731* dispersant	33
Raw talc milled in Isopar L[†] + 15 wt% Solsperse 2100[#] dispersant	33

* Orotan is an ICI surfactant based upon a sodium salt of a carboxylic acid copolymer.

[†] Isopar L, an Exxon chemicals product, is an isoparrafinic hydrocarbon with a chain length of $C_{12} - C_{15}$ and a specific boiling range.

[#] Solsperse 2100 is an ICI surfactant based on long chain alkyls

At a later stage of this work, the particle size of raw talc was also reduced by ultrasonicating approximately 50 wt% of raw talc in an aqueous mixture of H_2O and D_2O for 10 minutes. (Mixtures of H_2O and D_2O were required for the SANS contrast matching technique, the various proportions of H_2O/D_2O required were calculated and are given in Section 2.3.1). After ultrasonification, the sample was centrifuged at 1000 rpm and the supernatant liquid was extracted. This process was repeated approximately 12 times for each aqueous mixture. Each set of supernatants was combined and the excess liquid evaporated, to produce a wet 'sludge'. An exact amount of the required aqueous mixture was then added to each sludge to make up samples of 0.5 wt% fine talc. The talc content was confirmed to be 0.5 wt% by weight assays of these final solutions.

2.1.2 Guar Gum

Powdered guar gum samples were also provided by WMC Resources Ltd., and used without further processing.

2.2 Characterisation of Talc Prior to SANS

Scanning Electron Microscopy (SEM) was used to assess the morphology and particle size distributions of the various talc samples. The samples were prepared for SEM by evaporating dilute suspensions onto SEM sample holders; each sample received a thin carbon coating prior to placing in the microscope.

2.3 Contrast Matching Technique

In Small Angle Neutron Scattering (SANS) experiments the structure of a sample is probed by interactions between incident neutrons and the atomic nuclei composing the sample. The strength of these neutron-nuclear interactions is characterised by a property called 'scattering length', which is different for each isotope. Of particular advantage is the fact that the scattering lengths for hydrogen and deuterium are markedly different. The consequence of this is that solutions of H_2O and D_2O can be made up with the appropriate ratios to acquire a desired scattering length [7]. This is a powerful technique often used in SANS because it means that in a sample composed of two or more materials, the scattering length of one can be 'matched' to a solvent background of H_2O/D_2O, in essence, contrasting this particular material out of the final scattering pattern.

2.3.1 Scattering Length Density Calculations

For the contrast matching technique to be utilised in the present study, the scattering length densities (the scattering length of the molecule divided by molecular volume) of the sample components were calculated. The corresponding H_2O/D_2O mixture of identical scattering length density was then calculated. Details of these calculations are shown.

The scattering length densities (sld) of talc and guar gum molecules were calculated from the following equation,

$$\mathrm{sl}_{\mathrm{molecule}} = \sum \mathrm{sl}_{\mathrm{atom}}$$

$$\mathrm{sld} = \mathrm{sl}_{\mathrm{molecule}}/\mathrm{molecular\ volume}$$

Scattering lengths of individual atoms were obtained from standard tables [8]. The results of these calculations and the corresponding contrast match point with H_2O/D_2O solutions are shown in Table 3.

Table 3 – Calculated scattering length densities and corresponding contrast match points

Structure	sld (cm^{-2})	Contrast Match
Talc ($Mg_3Si_4H_2O_{12}$)	3.993×10^{10}	66% D_2O
Guar Gum ($C_4H_{20}O_{20}$)	6.843×10^{9}	18% D_2O
H_2O	-5.59×10^{9}	0% D_2O
D_2O	6.389×10^{10}	100% D_2O

However, XRD analysis of the raw talc, Table 1, demonstrates that these samples are not pure talc. They consist of approximately 56% talc and 44% impurities, mainly magnesite, hence the sld of magnesite was calculated as shown in Table 4 and the sld for raw talc modified according to these ratios.

Table 4 – Calculated scattering length densities and corresponding contrast match points for magnesite and talc

Material	sld (cm^{-2})	Contrast Match
Talc ($Mg_3Si_4H_2O_{12}$)	3.993×10^{10}	66% D_2O
Magnesite ($MgCO_3$)	6.33×10^{10}	99% D_2O
56% Talc + 44% Magnesite	5.02×10^{10}	79% D_2O

Calculation of the contrast match point for raw talc is obviously subject to some uncertainty because these samples consist of more than one mineral and the proportion of talc to magnesite might be slightly different for each sample prepared from the same batch. Also the plate like nature of talc particles causes the XRD data itself to have significant error since the grain orientation of these particles can significantly affect the percentages calculated. Considering these facts, it was decided that a contrast match of 80% D_2O (which is obviously easier to prepare than 79% D_2O) for talc would be sufficient for the experiments. Conversely, the calculations for the contrast match point for guar gum were a lot simpler because the guar gum is a pure homogeneous sample. Therefore, with the exception of preliminary work, all SANS experiments were conducted using a contrast match point of 80% D_2O for talc, and 18% D_2O for guar gum. Preliminary SANS experiments conducted at ANSTO using 18 and 80% D_2O demonstrated that these concentrations were sufficieint (within experimental error) to contrast out the guar gum and talc respectivley.

2.4 Small Angle Neutron Scattering (SANS) Experimental

2.4.1 SANS Sample Cells

Two types of sample cell were used in this work, the standard SANS cell and the rotational SANS cell. Initial experiments were conducted in standard SANS cells, which consist of 1 mm of sample sandwiched between two circular quartz windows of 1 mm thickness.

As the experiments proceeded, it became clear that the talc particles in a liquid environment required constant agitation to prevent sedimentation, which caused a reduction in concentration of suspended talc in the neutron beam.

In order to provide constant agitation, a rotational cell assembly was designed at ANSTO. The assembly contains a total of six sample cells, of the design shown in Figure 3. The sample aperture consists of two pieces of quartz clamped within a circular aluminum chamber. The sample to be studied was placed between the quartz windows in a manner similar to a standard SANS cell. The six chambers were placed in the cell assembly side by side so that the roughened edges were in contact. The cells in positions 3 and 4 of the assembly, were driven by a motor to rotate about the axis drawn at a constant rate. The contact between the roughened edges of the six cells ensures that the rotational motion was passed on to all the other cells in the assembly.

This assembly was tested for continuity of movement over a period of several days and the constant movement of the dispersed talc samples was found to be enough to prevent sedimentation of the powder during measurements.

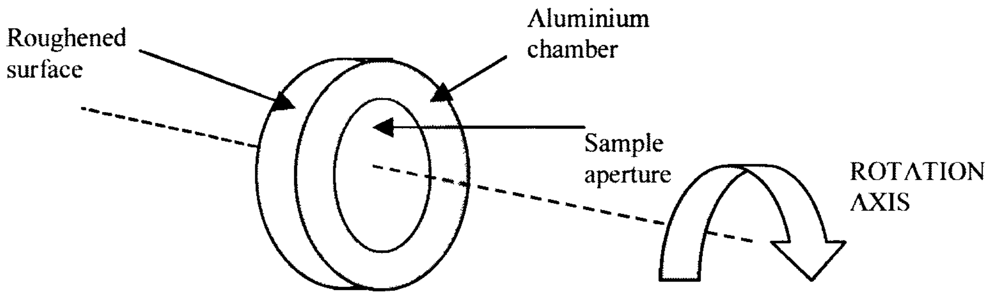

Figure 3 – As schematic of the rotational cell designed at ANSTO to provide constant agitation of suspended solids.

2.4.2 Measurement Procedure

Three different SANS instruments were used in this work, the SANS instrument at ANSTO, NG1 at NIST and NG3 at NIST. The instrument configurations are shown in the Appendix.

Precise weight percent solutions of talc, (raw or milled) and/or guar gum were made up in H_2O or D_2O solvents or a know mixture of H_2O/D_2O. These were immediately placed in the standard or rotational SANS cells as required and mounted in front of the beam aperture on the SANS instrument of choice. The neutron beam passed through the sample for the required sampling time and the intensity of scattered neutrons was recorded as a function of reciprocal space, 'q', at the He^3 detector.

Where; $q = [4\pi (\sin\theta)]/\lambda$
λ is the neutron wavelength
and 2θ is the angle of scatter

All of the intensities measured were normalised, that is corrected for any abnormalities in the detector matrix, scaled relative to the scattering from a porous silica standard and reported in units of cm^{-1} (cross section per unit volume).

The measured scattering intensity ($I_{measured}$) as function of 'q-space' was then corrected by the following process,

$$I_{correct} = [I_{measured} - I_{blocked\ beam}] - T_{sample}/T_{solvent\ cell}[I_{solvent\ cell} - I_{blocked\ beam}]$$

Where $I_{blocked\ beam}$ indicates the intensity of a signal recorded with the neutron beam blocked, this corrects the signal with respect to ambient background noise. $I_{solvent\ cell}$ is the measured scattering intensity recorded from a cell containing solvent only, this removes the scattering component in the measured signal which is directly attributed to the quartz windows and the solvent. $T_{sample}/T_{solvent\ cell}$ is the ratio of transmissions of the sample and a cell containing only solvent. The transmissions themselves are ratios of the neutron beam intensity with and without the presence of the sample or solvent cell.

The final signal was in 2 dimensional form, which was then circularly averaged to obtain a one-dimensional plot of scattering intensity verses q space.

2.4.3 Data Analysis

Where possible a standard fitting routine was used to obtain power law scattering coefficients from the averaged one dimensional data plots of I verse q. The program performs a least square fit of the data using the general expression $I(q) = Aq^{-P} + B$, where P is the power law coefficient. This expression is only true in the high q region of the scattering curves where Porod scattering dominates. The power law co-efficient can be interpreted in terms of the structure of the scattering object or surface [9].

3.0 Results and Discussion

3.1 Characterisation of Talc

Raw talc (Figure 4) contains some very large particles, (up to ~ 100 microns). Since these particles would not easily form stable suspensions and the large surface areas would dominate scattering behaviour, milling was carried out in an attempt to reduce the talc particle size. Surprisingly the milled samples still have a significant number of very large particles above ~ 10 μm (Figures 5 and 6). Also the talc milled in the presence of a dispersant (Figure 6) appears to agglomerate and clump together. Obviously milling increases the number of smaller particles but the fact that there is still a high population of large particles after milling means that they will continue to dominate SANS patterns.

It is interesting to compare the morphology of the raw and milled talc samples shown in Figures 4-6, because the raw talc itself has also been subject to crushing and ball milling in preparation for the flotation circuit by WMC. The cleavage planes on this talc however are much cleaner and more evident than those on the milled samples provided by CSIRO. This difference is attributed to the scale of milling processes, at CSIRO milling is carried out with zirconia beads of a diameter between 0.5 and 0.8 mm in comparison the smallest mill balls used by WMC are 42 mm in diameter. The larger scale milling would cause the ore to break up into relatively large pieces (100's of microns) primarily along natural cleavage planes, resulting in clean platelets. The small zirconia beads on the other hand cause much more damage to the surface of the cleavage planes as shown in Figures 5 and 6.

Figure 4 – SEM micrograph of raw unmilled talc

Figure 5 – SEM micrograph of talc milled in water with no dispersant

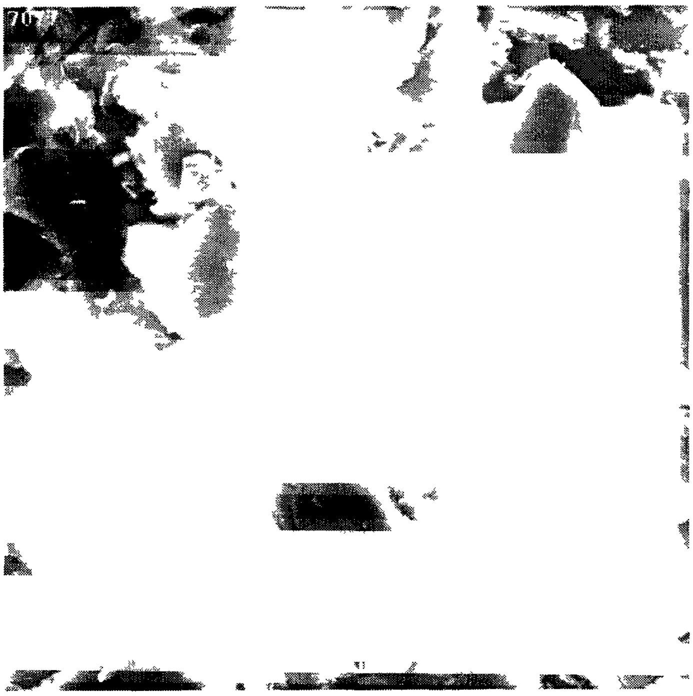

Figure 6 – SEM micrograph of talc milled in water with Orotan dispersant

3.2 Preliminary SANS Results

Preliminary SANS experiments were conducted at NIST using the milled samples in standard (non rotating cells). A number of observations were important in determining the subsequent direction of the SANS work.

Firstly, it was observed that the milled (milled in water with or without dispersant) talc particles always scattered with a power law coefficient close to -3.0. Co-efficients between –3.0 and –4.0 are indicative of fractally rough surfaces [9]. This observation correlates with the SEM micrographs shown in Figures 5 and 6.

It was also noted that the milled samples did not remain dispersed during the course of the experiments, even when the milled samples contained dispersant from the milling process. (The term dispersant is misleading here since the dispersant is added at the milling stage to lower the viscosity and increase the efficiency of the milling process and not to form stable dispersions).

From these observations the following directives were followed:

1) Even though SANS data was retrieved from these initial experiments it became clear that even the milled talc samples did not form stable suspensions. The particles either settled to the base of the sample holder or floated to the top on the surface of any air bubbles. Both of these mechanisms meant that the concentration of talc observed in the beam at any one time is unlikely to be the initial concentration placed in the cell. This was overcome in future work by the use of the rotational cell described in the experimental section.

2) SEM and initial SANS experiments both indicate that the surface of the milled talc has been roughened substantially, without significantly reducing the number of very large particles. This surface roughening reflects lattice distortions and surface defects which would be expected to upset the natural hydrophobic/hydrophilic balance of the mineral [3]. The presence of the organic dispersants in the system also adds another variable to an already complex system. Therefore it was decided that future SANS experiments would only be conducted on the raw talc samples, because of the 'clean' nature of their cleavage planes, and the absence of adsorbed organics.

3.3 Verification of Contrast Match Points

A series of experiments on NG1 were conducted with 2wt% talc and 2wt% guar gum solutions in various H_2O/D_2O mixtures to establish the accuracy of the calculated contrast match points. The I verse q curves for these experiments are shown in Figures 7 and 8.

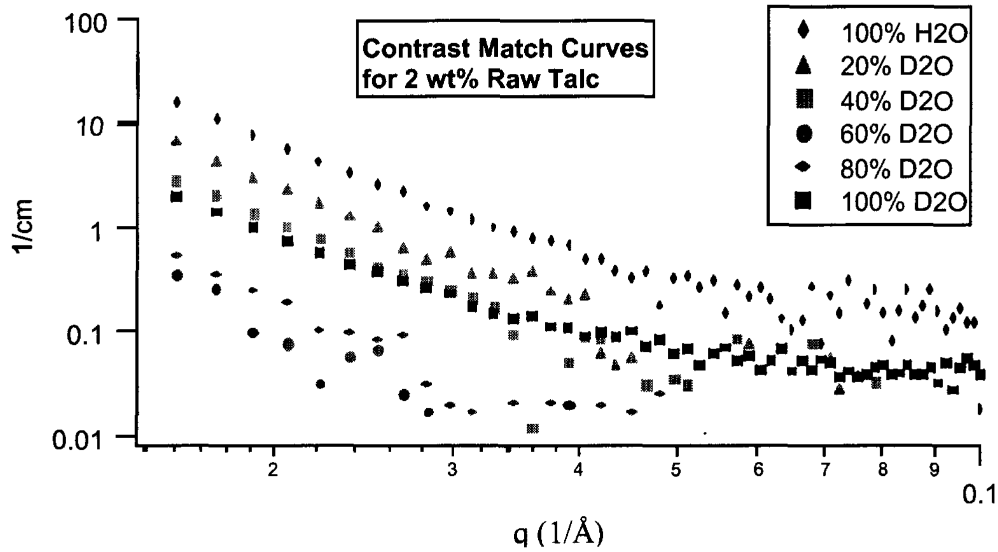

Figure 7 – Scattering curves for 2 wt% raw talc samples in various H_20/D_2O mixtures used to determine the contrast match point for raw talc

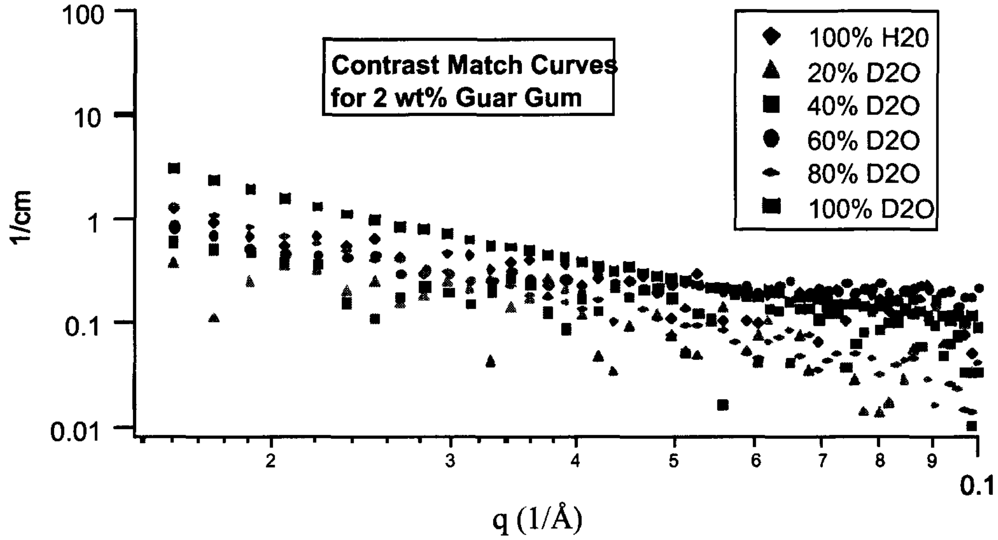

Figure 8 – Scattering curves for 2 wt% guar gum samples in various H_20/D_2O mixtures used to determine the contrast match point for guar gum

From the I verse q curves shown in Figures 7 and 8, the scattering intensity at q=0 was extrapolated, (I(q=0)). The square root of this value plotted against %D_2O enables an experimental determination of the contrast match point for each material. These plots are shown in Figures 9 and 10. It can be seen that a linear curve fit yields a percentage of D_2O which can be interpreted as the contrast match point for the material being studied. It is clear then that the calculated contrast match points of 18% D_2O for guar gum and 79% D_2O for raw talc are close to the experimentally determined values. The discrepancy (71.49% as compared to 79% D_2O) in the measured and calculated match point for talc could easily be attributed to the fact that this material is not pure and the sld might vary from experiment to experiment owing to differing amounts of contaminants.

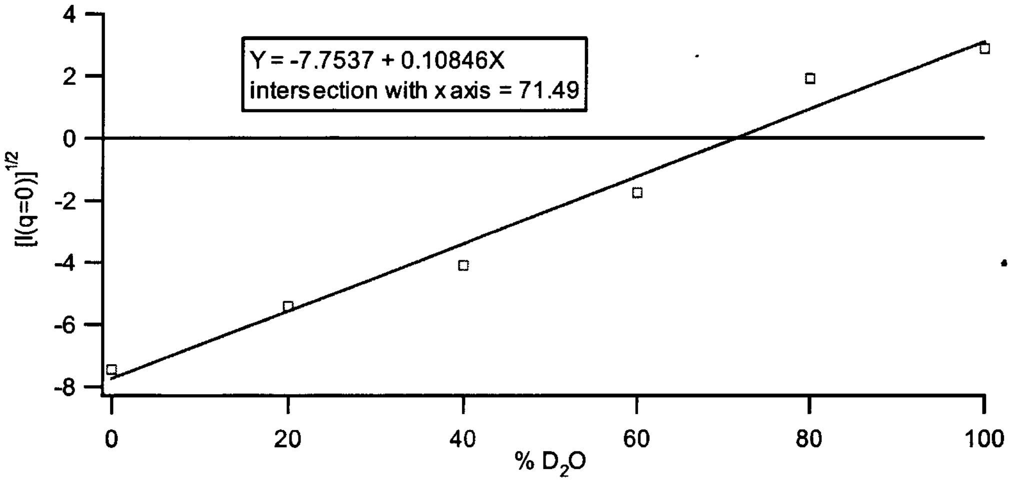

Figure 9 - Plot of √I(q=0) verses % D_2O, for raw talc, intersection with the x-axis indicates the contrast match point for raw talc

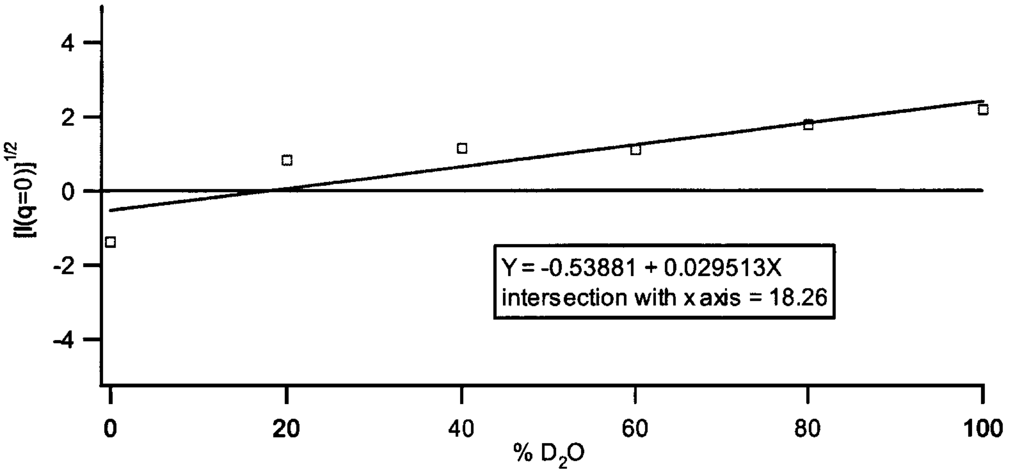

Figure 10 - Plot of √I(q=0) verses % D_2O, for guar gum, intersection with the x-axis indicates the contrast match point for guar gum.

3.4 SANS Study of Talc and Guar Gum Interactions

3.4.1 Experiments Conducted at ANSTO

A study of the interactions of guar gum and raw unmilled talc was undertaken on the SANS instrument at ANSTO. The instrument configuration used is described in the Appendix.

Initially scattering from solutions of guar gum alone were studied in order to assess the strength of the scattering from this polymer. The scattering intensity as a function of guar gum concentration is shown in Figure 11. From this it is clear that a concentration of at least 0.5 wt% guar gum is required to obtain measurable scattering intensity.

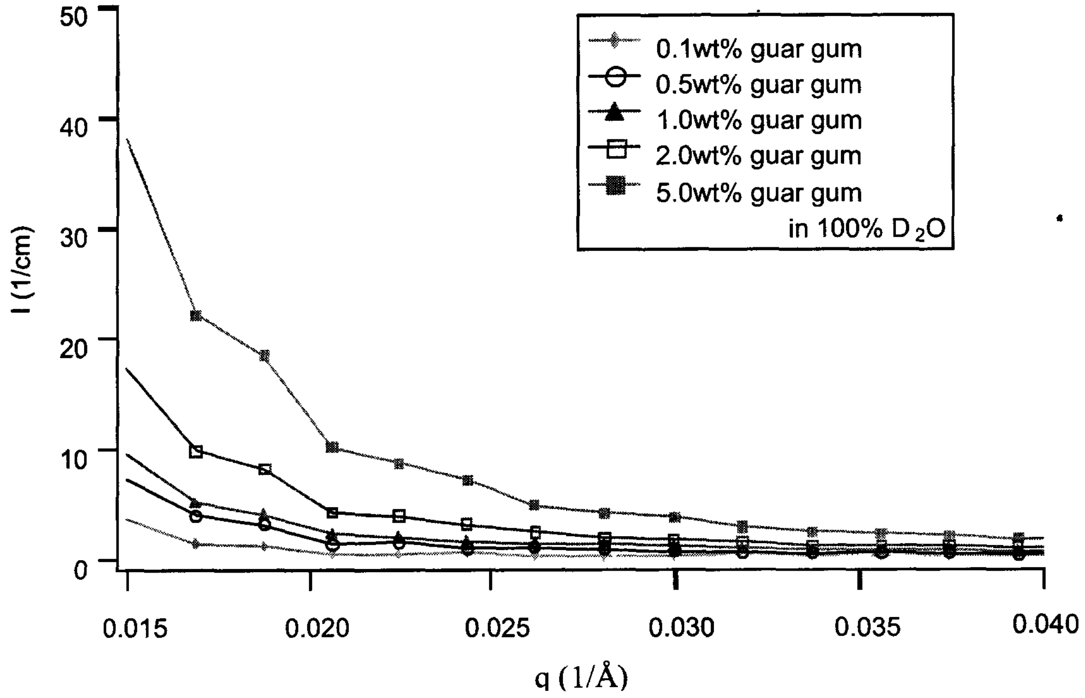

Figure 11 – Scattering curves of guar gum as a function of concentration in 100% D_2O

Once the concentration of guar gum required was established a series of experiments was carried out in the rotational cell with raw unmilled talc on the SANS instrument at ANSTO using the sample set described in Table 5.

Table 5 – The sample set used in SANS experiments at ANSTO to investigate interactions between talc and guar gum

Sample description	Contrast Match Point	Scattering From
1 wt% raw talc +1 wt% guar gum in 18% D_2O	Guar gum	Raw Talc
1 wt% raw talc in 18% D_2O	Guar gum	Raw Talc
1 wt% raw talc + 1 wt% guar gum in 80% D_2O	Raw talc	Guar gum
1 wt% guar gum in 80% D_2O	Raw talc	Guar gum

By using solvent ratios of 18% D_2O and 80% D_2O, it should be possible to study the scattering of talc with and without the presence of guar gum and the scattering of guar gum with and without the presence of talc respectively. The results are presented in Figures 12 and 13.

The curves in Figure 12, in 18% D_2O, (the contrast match point for guar gum) suggest that the talc particles scatter in the same manner either with or without the presence of guar gum. Conversely, the curves in Figure 13, in 80% D_2O, (the contrast match point for talc) demonstrate a change in the scattering behaviour of guar gum when talc is also present in the solution. The presence of talc increases the scattering intensity, indicating that the guar gum is taking on a new morphology, probably as a coating on the talc. The guar gum consists of very long chain polymer molecules. The scattering from these 'free chains' suspended in solution would be expected to be quite different from the scattering observed when the chains are adsorbed onto the surface of talc particles.

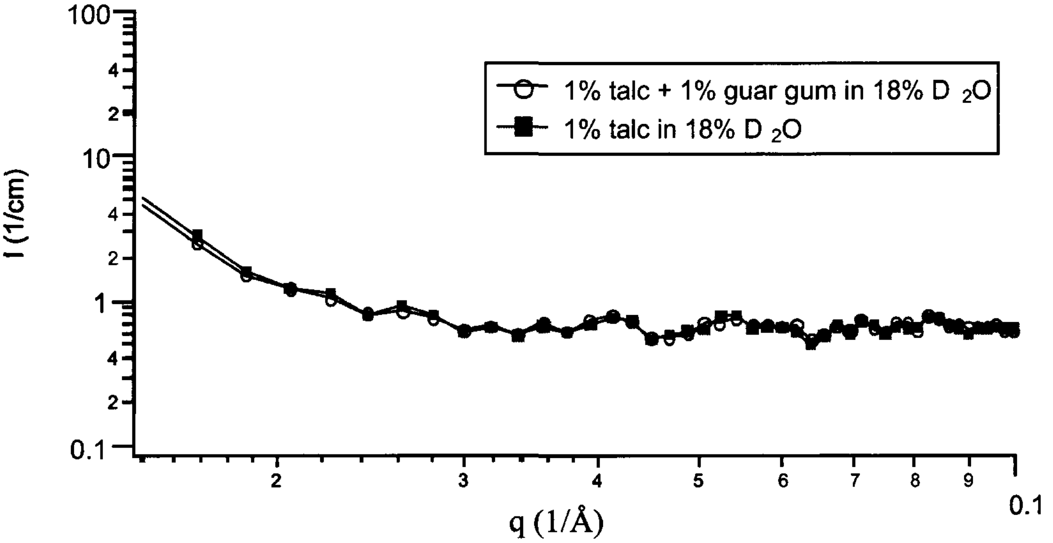

Figure 12 – Scattering curves from 1 wt% raw talc in 18% D_2O solutions with and without the presence of guar gum, recorded on the SANS at ANSTO

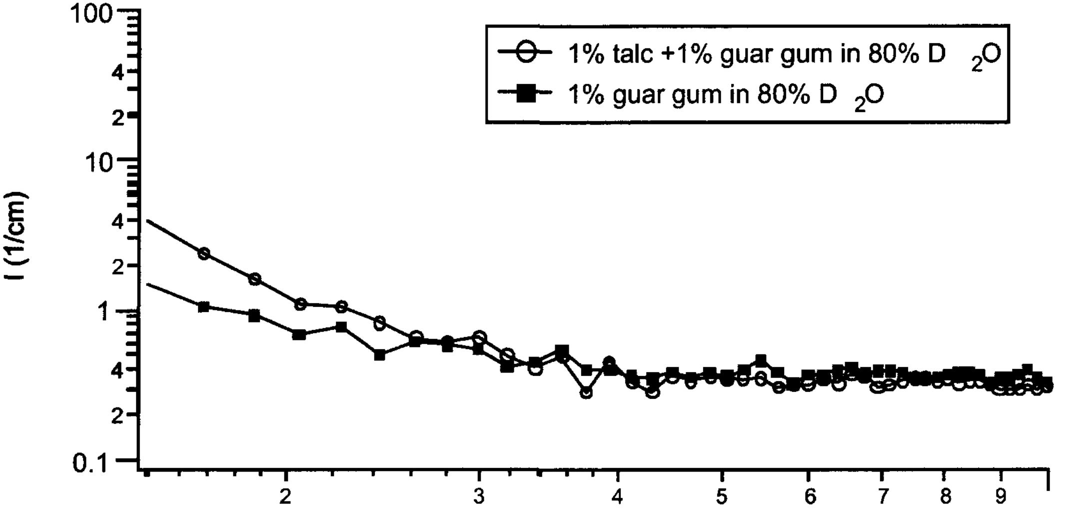

Figure 13 – Scattering curves from 1 wt% guar gum in 80% D_2O solutions with and without the presence of raw talc, recorded on the SANS at ANSTO

As a matter of interest, the power law co-efficients were calculated as described in Section 2.4.4. Since this fitting routine is applied to a limited q range, the coefficients can be viewed as a useful indication of the structures causing scattering but are not irrefutable proof of such structures. The calculated coefficients are shown in Table 6.

Table 6 – Power Law coefficients calculated from data in Figures 12 and 13

Sample	Power Law Co-efficient (P)
1 wt% talc + 1 wt% guar gum in 18% D_2O	-3.97
1 wt% talc in 18% D_2O	-4.18
1 wt% guar gum in 80% D_2O	-2.23
1 wt% talc + 1 wt% guar gum in 80% D_2O	-3.78

The SANS instrument at ANSTO has a q range of 0.01 to 0.1 1/Angstroms, equivalent to a length scale of 0.06 to 0.0062 microns. Considering that the talc particles range from a few tens of a micron to hundreds of microns in size, any scattering caused by talc can be assumed to be due to surface scattering and not due to scattering from individual particles. In the Porod region a power law co-efficient of -4.0 indicates scattering from smooth surfaces [9]. This is interesting to compare to the power law coefficients measured for milled talc which were always close to –3.0, indicating fractally rough surfaces [9]. Thus the scattering curves emphasize the different surface properties of the milled and unmilled talc.

It can be seen that the guar gum power law co-efficient changes in the presence of talc (from -2.23 to -3.78) even though the talc is contrasted out at 80% D_2O. It is reasonable to assume that this is due to the guar gum coating the talc particles and hence taking on a new structural form.

The fact that the raw talc samples contains such large particles means that the scattering patterns described are dominated by the behaviour of these very large particles. It was decided that the talc particle size should be reduced and scattering experiments repeated over a much wider q range in an attempt to obtain additional information about the adsorption of guar gum on talc surfaces. For this purpose fine talc samples were prepared and the experiments repeated at NIST.

3.4 SANS Study of Talc and Guar Gum Interactions

3.4.2 Experiments Conducted at NIST

The experiments discussed above were repeated on NG1 and NG3, except that very fine dispersions of talc were used, which were prepared by repeated centrifuging and ultrasonicating, as described in the experimental section. This method of preparing the fine particle samples depends upon particle size separation rather than particle fracture as in the case of ball milling. As such this method would not be expected to cause a huge increase in surface roughness or defects during the process, unlike milling methods.

NG1 has a similar q range to the SANS instrument at ANSTO, which is approximately 0.01 to 0.1 1/Angstroms, equivalent to a length scale of 0.06 to 0.0062 microns. NG3 has a q range of 0.002 to 0.01 1/Angstroms, equivalent to a length scale of 0.3 to 0.06 microns. The instrument configurations used for NG1 and NG3 are described in more detail in the Appendix.

The scattering curves from NG1 and NG3 have been compiled onto the same I verse q curves in Figures 14 and 15. Some adjustment in the background scattering of the NG3 data was required to enable the curves to align.

The scattering behaviour of the fine talc in 18% D_2O solutions, which are contrast matched to guar gum, are shown in Figure 14. From these curves it is clear that there is a slight increase in scattering intensity over the entire q range when guar gum is also present. This behaviour is especially pronounced at a q range from 0.01 to 0.02 $Å^{-1}$. This is curious because on the ANSTO instrument there was no change in talc scattering function or intensity over this q range caused by the presence of guar gum.

Since all samples were prepared in the same way immediately prior to the SANS experiments these changes in scattering behaviour cannot be attributed to discrepancies caused by sample preparation.

The most likely cause of this discrepancy would stem from the fact that the scattering at ANSTO was on raw talc and the scattering behaviour was dominated by scatter from the surface of large particles. However, at NIST, the talc was of a much finer particle size, due to its more sophisticated preparation. Further work on the fine talc system would be required to establish the reproducibility of this behaviour before a more detailed explanation can be proposed.

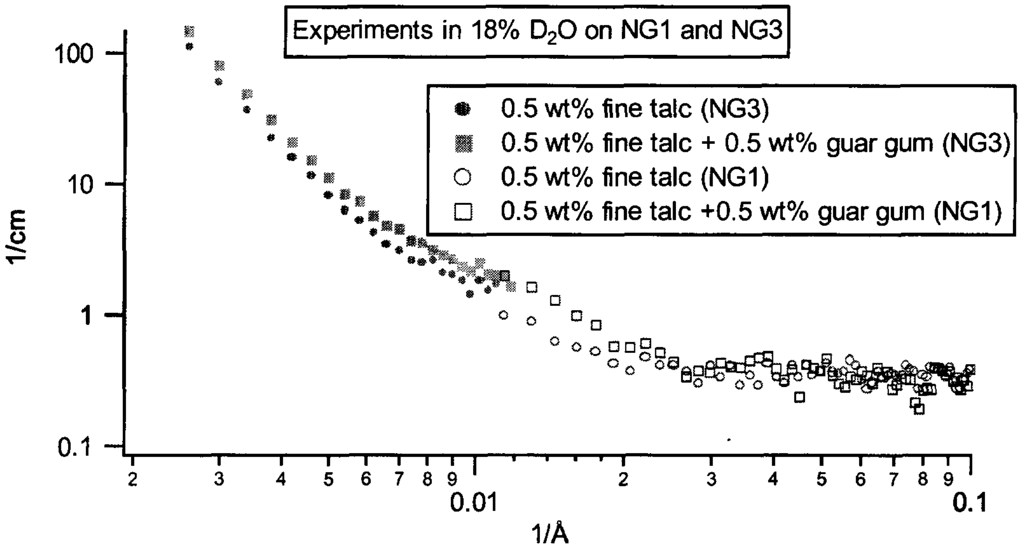

Figure 14 – Scattering curves from 0.5 wt% fine talc in 18% D_2O solutions with and without the presence of guar gum, recorded on NG1 and NG3 at NIST

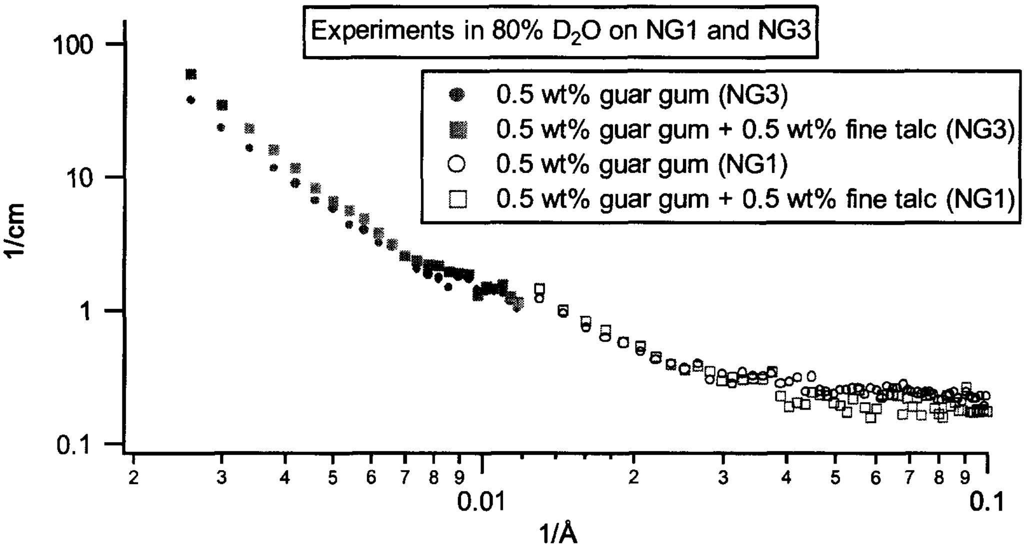

Figure 15 – Scattering curves from 0.5 wt% guar gum in 80% D_2O solutions with and without the presence of fine talc, recorded on NG1 and NG3 at NIST

The scattering intensity of guar gum in the presence of talc, observed on the ANSTO instrument, increased compared to its scattering without the presence of talc (Figure 13). The results on NG1 and NG3 at NIST also show an increase in scattering intensity, but only at low q (Figure 15).

The scattering behaviour from raw talc recorded at ANSTO is evidently due to scattering from the surface of the large particles. Consequently the changing scatter of guar gum in the presence of this raw talc is readily attributed to interactions with the talc surface.

In SANS measurements at NIST the size of the particles is reduced and the q range increased, this causes the scattering of talc to be a mixture of surface and mass scattering. Even so the increased scatter of guar gum in the presence of talc implies that the guar gum has taken on a more ordered structural form. Taking into account the results from ANSTO it is feasible that this structural order is brought about by the adsorption of the guar gum onto the talc particles. The shift in q range is probably due to the difference in talc particle size since this is the major difference between the samples observed at ANSTO and NIST.

The nature of the talc sample in the present study, most notably the poly dispersity of particle sizes and the presence of impurities makes it difficult to model the surface interactions of guar gum and talc. In order to extricate all of the factors involved and thus provide a more complete description of the adsorption behaviour of guar gum on talc more homogeneous solutions must be studied.

4.0 Conclusion

Combined SANS experiments at ANSTO and NIST have been utilised to investigate the interactions of talc and guar gum in aqueous based suspensions. The size of the talc particles appears to effect the scattering behaviour not only of talc but also of guar gum in the same solutions. This implies that the structure of the guar gum is strongly influenced by the dimensions of the talc and could be taken as indirect evidence of adsorption of guar gum onto the talc surface.

Although adsorption has been implied, a model of the adsorption mechanism cannot be proposed from these preliminary results. In order to achieve this, more homogeneous talc samples need to be studied; in particular the poly dispersity of and impurities in the samples must be addressed.

This project was a pioneering study using SANS in collaboration with Australian industry. The results presented here suggest that further studies focussed on particular components of this system could clarify the adsorption mechanism between talc and guar gum. In a more generic sense, this report demonstrates that Small Angle Neutron Scattering can be used as an applied technique to study interactions between organic and inorganic materials in liquid environments reflecting their behaviour in complex industrial systems.

Appendix - Instrument Configurations

Table A1- SANS Instrument Configuration ANSTO

Source Aperture Diameter	3.0 cm
Source Aperture to Sample Aperture Distance	500 cm
Sample Aperture to Detector Distance (SDD)	500 cm
Beam Diameter	1cm
Beam Stop Diameter	4.5 cm
Minimum Q-value	0.01 Å^{-1}
Maximum Q-value	0.1 Å^{-1}
Sample Aperture Diameter	1 cm
Detector Centre Offset	0
Neutron Wavelength	3.5 Å
Wavelength Spread (FWHM)	0.15

Table A2- NG1 Instrument Configurations NIST

Source Aperture Diameter	2.54 cm
Source Aperture to Sample Aperture Distance	410 cm
Sample Aperture to Detector Distance (SDD)	360 cm
Beam Diameter	0.95 cm
Beam Stop Diameter	5.7 cm
Minimum Q-value	0.01 Å^{-1}
Maximum Q-value	0.1 Å^{-1}
Sample Aperture Diameter	0.95 cm
Detector Centre Offset	0
Neutron Wavelength	6 Å
Wavelength Spread (FWHM)	0.14

Table A3- NG3 Instrument Configurations NIST

Source Aperture Diameter	2.54 cm
Source Aperture to Sample Aperture Distance	1632 cm
Sample Aperture to Detector Distance (SDD)	1310 cm
Beam Diameter	5.07 cm
Beam Stop Diameter	5.08 cm
Minimum Q-value	0.0021 Å^{-1}
Maximum Q-value	0.0262 Å^{-1}
Sample Aperture Diameter	1.27 cm
Detector Centre Offset	0
Neutron Wavelength	6 Å
Wavelength Spread (FWHM)	0.150

Acknowledgements

The authors would like to acknowledge John Rumball from WMC Mineral Processing Group for providing talc and guar gum samples and information about the Leinster Nickel Operations, in particular the flotation process. We would also like to acknowledge Anne Bayada and Terry Turnie of CSIRO, Division of Manufacturing Science and Technology for milling the talc samples and for their helpful discussions regarding talc properties and the milling process.

References

[1] M.C. Fuerstenau, A. Lopez-Valdivieso and D.W. Fuerstenau, Int. J. Mineral Proc., 23, (1988), 161-170

[2] J. McHardy and T. Salman, Transactions of the Institute of Mining and Metallurgy, SectionC, v83, n808, 1974, ppc25-c29.

[3] R.J. Pugh, Int. J. Mineral Proc., 25, (1989), 101-130

[4] Discussions with Dr. John Rumball, Mineral Processing Group, WMC Resources Ltd., Perth, WA

[5] MSDS of Guar Gum, ChemWatch, March 2000.

[6] J.M.W Mackenzie, E&MJ, October, (1980), 80-87

[7] J.S. Higgins and H.C Benoit, in 'Polymers and Neutron Scattering', Oxford University Press Inc., New York, 1996.

[8] CRC Handbook of Chemistry and Physics, Ed. D.R. Lide, 75th Ed., CRC Press Inc., 1994

[9] D.W. Schaefer, J.E. Martin and K.D. Keefer in 'Physics of Finely Divided Matter', eds. N. Bocarra and M. Daoud (Springer-Verlag, Berlin, 1985), p.31.